nature cell biology

The thioredoxin-related redox-regulating protein nucleoredoxin inhibits Wnt–β-catenin signalling through Dishevelled

Yosuke Funato[1,2], Tatsuo Michiue[3], Makoto Asashima[3,4] and Hiroaki Miki[1,5,6]

Dishevelled (Dvl) transduces signals from the Wnt receptor, Frizzled, to downstream components, leading to the stabilization of β-catenin and subsequent activation of the transcription factor T cell factor (TCF) and/or lymphoid enchancer factor (LEF)[1–3]. However, the mechanism of Dvl action remains unclear. Here, we report that nucleoredoxin (NRX)[4], a thioredoxin (TRX) family protein, interacts with Dvl. Overexpression of NRX selectively suppresses the Wnt–β-catenin pathway and ablation of NRX by RNA-interference (RNAi) results in activation of TCF, accelerated cell proliferation and enhancement of oncogenicity through cooperation with mitogen-activated extracellular signal regulated kinase kinase (MEK) or Ras. We find that cells respond to H_2O_2 stimulation by activating TCF. Redox-dependent activation of the Wnt–β-catenin pathway occurs independently of extracellular Wnts and is impaired by RNAi of NRX . In addition, association between Dvl and NRX is inhibited by H_2O_2 treatment. These data suggest a relationship between the Wnt–β-catenin pathway and redox signalling through redox-sensitive association of NRX with Dvl.

The Wnt signalling pathway is evolutionarily conserved from nematodes to mammals[1–3]. The Wnt ligands bind to the Frizzled receptor and induce the cytosolic accumulation of β-catenin by inhibiting the β-catenin destruction complex (composed of Axin, adenomatous polyposis coli (APC) and GSK3β). Accumulated β-catenin migrates to the nucleus and activates the transcription factor TCF. Dvl is crucial in this process, but its mechanism of action is unknown.

TRXs are members of a family of evolutionary conserved proteins that possess catalytically active cysteine residues that can reduce the disulphide bonds of target proteins[5]. One well-known target is peroxiredoxin[6], which scavenges reactive oxygen species (ROS). In addition to its catalytic activity, TRX binds and regulates Ask1, a MAP kinase kinase kinase (MAPKKK) involved in apoptosis[7]. Stimulating cells with H_2O_2 leads to oxidation of TRX, which results in dissociation from Ask1.

To determine the role of Dvl, an *in vivo* search for Dvl binding partners was performed. An NIH3T3 murine fibroblast-derived cell line that stably expressed FLAG-tagged Dvl1 was generated. Immunoprecipitation with anti-FLAG antibodies pulled down several proteins that were identified by silver staining (Fig. 1a) and mass spectrometry analysis. The major band was identified as NRX, a TRX family member, which was previously reported to localize to the nucleus[4]. Dvl mainly exists in the cytoplasm, therefore anti-NRX antibodies were generated to analyse the subcellular localization of NRX. A positive NRX signal was found only in the cytosolic fraction, indicating that NRX exists predominantly in the cytosol (see Supplementary Information, Fig. S1a, b).

Immunoprecipitation analyses confirmed endogenous complex formation between Dvl and NRX. A positive Dvl signal was identified in anti-NRX precipitates but not in precipitates with control rabbit-IgG or anti-NRX antibodies preincubated with GST–NRX (Fig. 1b). Coimmunoprecipitation of ectopically expressed Myc–Dvl1 was also observed with FLAG–NRX (Fig. 1c). A mobility shift of Myc–Dvl1, due to altered phosphorylation of Dvl, was identified when FLAG–NRX was coexpressed (see Supplementary Information, Fig. S1c), suggesting a possible role for NRX in the regulation of Dvl. Expression of a catalytic-deficient mutant of NRX ($NRX^{C205S/C208S}$, denoted hereafter as NRX-Mut) caused little mobility shift of Myc–Dvl1, and FLAG–NRX-Mut did not coprecipitate with Myc–Dvl1 (Fig. 1c).

The region of Dvl involved in the interaction with NRX was then determined. Pull-down assays with deletion constructs of Myc–Dvl1 and GST–NRX revealed that the basic–PDZ domain (PDZ, PSD95–Dlg–ZD1) of Dvl1 is the minimum region essential for binding to NRX (see Supplementary Information, Fig. S1d, e). The direct interaction between recombinant Dvl1 and NRX proteins was also analysed. Pull-down assays were performed with purified GST–Dvl1–PDZ–DEP–His (DEP, Dishevelled–Egl10–Pleckstrin; includes the basic–PDZ domain) and His–NRX under various redox conditions (as NRX belongs to the TRX redox catalytic family) and it was observed that the Dvl–NRX interaction was clearly lessened by altering the reactive cysteine residues

[1]Division of Cancer Genomics and [2] Division of Biochemistry, Institute of Medical Science, University of Tokyo, 4-6-1 Shirokanedai, Minato-ku, Tokyo 108–8639, Japan. [3]Department of Life Sciences (Biology), Graduate School of Arts and Sciences, University of Tokyo, 3-8-1, Komaba, Meguro-ku, Tokyo 153–8902, Japan. [4]ICORP, Japan Science and Technology Agency (JST), 3-8-1, Komaba, Meguro-ku, Tokyo 153-8902, Japan. [5]PRESTO, JST, 4-1-8 Honcho, Kawaguchi-shi, Saitama 332–0012, Japan. [6]Correspondence should be addressed to H.M. (e-mail: miki@ims.u-tokyo.ac.jp)

Received 9 November 2005; accepted 13 March 2005; published online 2 April 2006; DOI: 10.1038/ncb1405

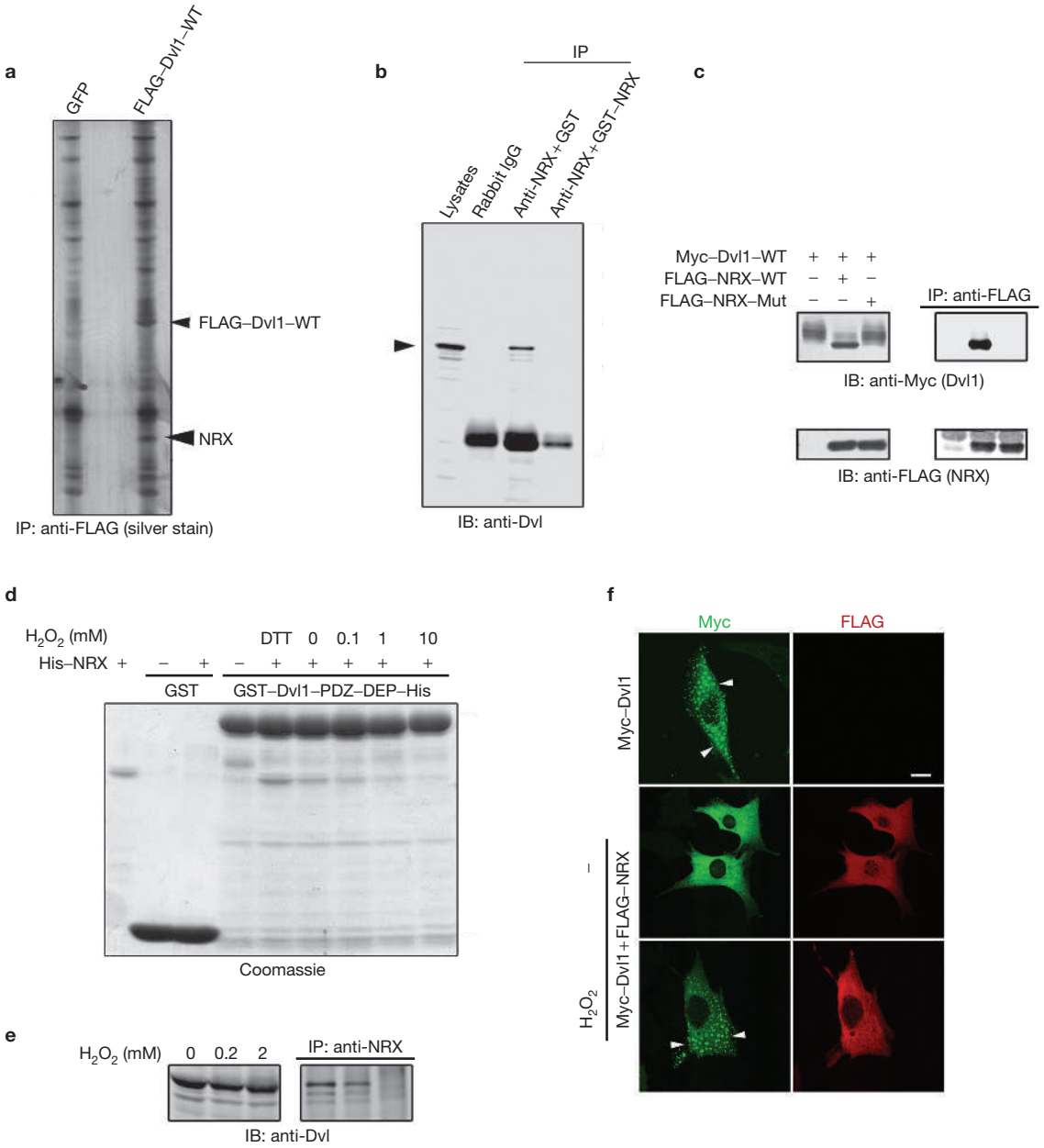

Figure 1 Redox-dependent association between Dvl and NRX. (**a**) Anti-FLAG immnuoprecipitation (IP) with a stable FLAG–Dvl1 clone. (**b**) Immunoprecipitation of lysates from L cells by anti-NRX (preincubated with GST or GST–NRX). Arrowhead indicates endogenous Dvl. (**c**) Immunoprecipitation of expressed FLAG–NRX (wild-type (WT) and mutant (Mut)) and Myc–Dvl1. (**d**) GST pull-down assays with GST–Dvl1–PDZ–DEP–His and His–NRX under reduced (1 mM DTT) or oxidized (H_2O_2) conditions. (**e**) Anti-NRX immunoprecipitation of L cell lysates treated with H_2O_2 (30 min). (**f**) Transfected NIH3T3 cells treated with 1 mM H_2O_2 for 1 h. Red: anti-FLAG (NRX), Green: anti-Myc (Dvl1). Arrowheads indicate Myc–Dvl1 that shows punctate localization. Scale bar represents 5 μm.

(Fig. 1c). Coomassie brilliant blue (CBB) staining showed direct interaction between Dvl1 and NRX, and the amount of Dvl1-bound NRX increased under reduced conditions (with diothreitol) and decreased with oxidation by H_2O_2 (Fig. 1d). Pull-down assays were also performed with Dvl1 or NRX that were separately treated with H_2O_2. The amount of bound NRX decreased when NRX was treated with H_2O_2, but not when Dvl1 was treated with H_2O_2, suggesting that NRX selectively responds to oxidative stress (see Supplementary Information, Fig. S1f). The interaction between endogenous Dvl and NRX was examined to determine whether it is also redox-dependent. The amount of coimmunoprecipitated Dvl decreased with H_2O_2 treatment (Fig. 1e). Expressed Myc–Dvl1 showed a punctate localization in cells (Fig. 1f and several previous reports[8]). In response to FLAG–NRX coexpression, Myc–Dvl1 localization became diffuse within the cytosol, but punctate localization was clearly restored by H_2O_2 treatment (Fig. 1f). Taken together, these data indicate that Dvl and NRX form an *in vivo* complex and that their interaction is regulated by oxidative stress.

We next examined the possible role of NRX in activation of TCF using luciferase reporter gene expression assays. Myc–Dvl1-expressing cells showed approximately sevenfold stimulation of expression compared with that of cells transfected with empty vector. This expression was completely suppressed by coexpression of wild-type Myc–NRX but not

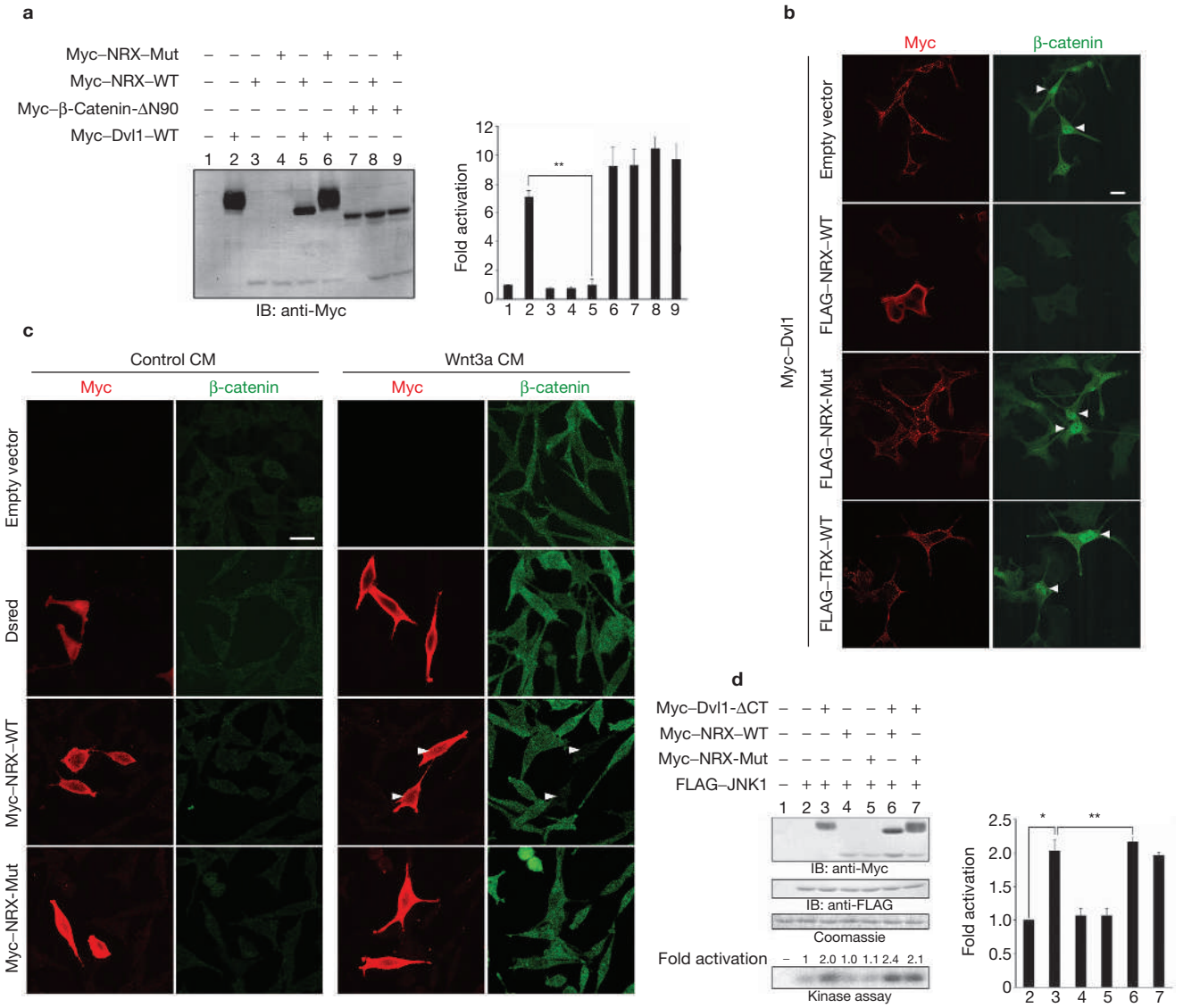

Figure 2 NRX suppresses Wnt–β-catenin signalling. (**a**) Reporter gene expression assays in HEK293 cells. A representative immunoblot is indicated. The error bars indicate the mean ± s.e.m ($n = 3$) and the asterisks indicate $P = 0.0062$. (**b**) N1E-115 cells transfected with the indicated constructs and visualized by anti-Myc (Dvl1; red) and anti-β-catenin (green) staining. Arrowheads indicate accumulated β-catenin. (**c**) L cells transfected with the indicated constructs and treated with Wnt3a conditioned medium (CM) or control CM. Arrowheads indicate cells expressing Myc–NRX–WT. (**d**) Kinase assays against GST–c-Jun (1–79) with anti-FLAG immunoprecipitates of transfected COS7 lysates. Representative results of the kinase assay and immunoblot analysis are indicated. The error bars indicate the mean ± s.e.m ($n = 3$) of the kinase assay. Single asterisk indicates $P = 0.010$; double asterisk indicates $P = 0.51$. Scale bars represent 5 μm in **b** and **c**.

of Myc–NRX-Mut (Fig. 2a). NRX coexpression did not suppress activation induced by ΔN90-β-catenin, a dominant-active form of β-catenin[9]. Coexpression analysis was performed in N1E-115 neuroblastoma cells to directly investigate β-catenin stabilization. Myc–Dvl1 expression induced significant accumulation of β-catenin (Fig. 2b). Coexpression of wild-type FLAG–NRX, but not of FLAG–NRX-Mut, clearly suppressed accumulation. Coexpression of FLAG–TRX did not inhibit β-catenin accumulation, suggesting that the inhibitory effect of NRX is not due simply to altered redox conditions within the cells. We then tested whether NRX can inhibit Wnt–β-catenin signalling induced by Wnt ligands. L cells were treated with Wnt3a conditioned medium (Wnt3a CM) and a significant accumulation of β-catenin was induced (Fig. 2c), which was clearly suppressed in cells expressing wild-type Myc–NRX.

Dvl activates not only the Wnt–β-catenin pathway but also c-Jun NH2-terminal kinase (JNK) in a manner independent of β-catenin accumulation[10,11]. Therefore, the possible role of NRX in Dvl-induced activation of JNK was also analysed. Myc–Dvl1-ΔCT (Dvl1 lacking the carboxy (C)-terminal region) was transfected to enhance the kinase activity of JNK but no significant effect of wild-type Myc–NRX coexpression was observed (Fig. 2d). Myc–Dvl1-ΔCT was used instead of wild-type Myc–Dvl1 because of a report that Dvl lacking the C-terminal region exerts a stronger effect on JNK stimulation than wild-type Dvl[10]. A similar tendency was also observed when wild-type Myc–Dvl1 was transfected (data not shown). Thus, NRX appears to be a specific suppressor of Wnt–β-catenin signalling.

NRX binds to the basic–PDZ domain of Dvl but may compete with other binding proteins to interact with this region. One possible

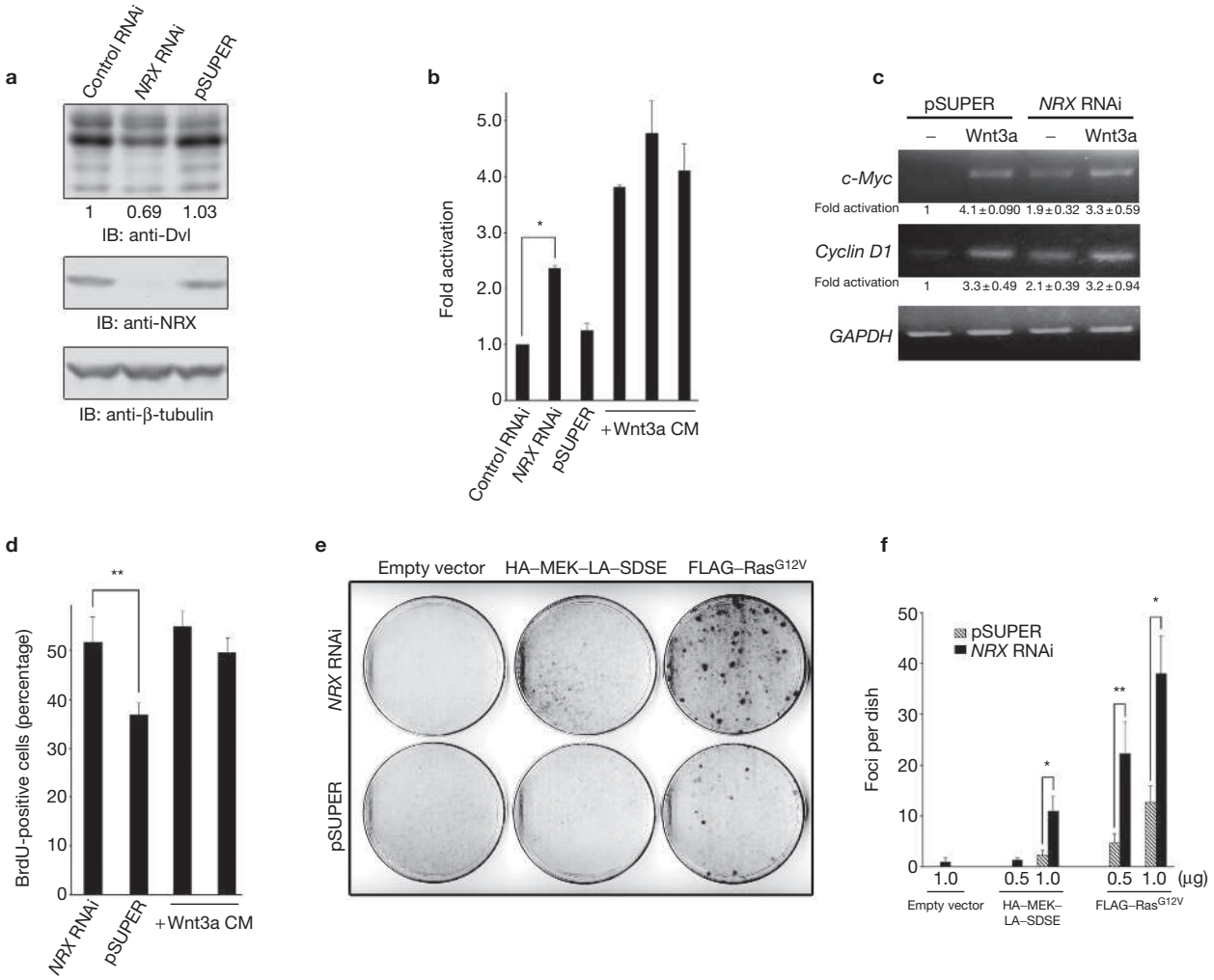

Figure 3 *NRX* RNAi shows TCF activation and increased cell proliferation. (**a**) NIH3T3 cells were infected with retroviruses for vector (pSUPER), *NRX*, or control RNAi. The relative amount of Dvl is shown. (**b**) TCF reporter activities in the presence or absence of Wnt3a conditioned medium (CM) are indicated. Results are shown as the the mean ± s.e.m ($n = 3$). Asterisk indicates $P=0.018$. (**c**) RT–PCR analyses of c-Myc and Cyclin-D1 are indicated. The mean ± s.e.m ($n = 5$) of relative amount of product are also shown. (**d**) The rates of BrdU-incorporation are shown as the mean ± s.e.m ($n = 5$). Double asterisk indicates $P=0.0055$. (**e**) Representative result of transformation assays with transfected *NRX* RNAi cells. Foci are visible as black dots in each dish. (**f**) Numbers of foci generated in each dish. Results are shown as the mean ± s.e.m ($n = 3$). Single asterisk indicates $P=0.027$; double asterisk indicates $P=0.041$.

competitor is Frat, an activator of Wnt–β-catenin signalling[12,13]. Pull-down assays were performed with recombinant Dvl1, NRX and Frat1. Binding of His–Frat1 to GST–Dvl1–PDZ–DEP–His was inhibited by His–NRX (see Supplementary Information, Fig. S2a). Competition between Frat and NRX was also observed *in vivo*. Myc–Frat1 coimmunoprecipitation with FLAG–Dvl1 was reduced by Myc–NRX coexpression (see Supplementary Information, Fig. S2b). The competition between NRX and Frat for interaction with Dvl was blocked by H_2O_2 treatment; the amount of NRX bound to Dvl1 decreased in the presence of H_2O_2; in contrast, more Frat1 bound to Dvl1 in these conditions (see Supplementary Information, Fig. S2c). The cellular localization of Frat1 was also examined. GFP–Frat1 was observed throughout the cytosol. Coexpression of Myc–Dvl1 induced punctate localization of GFP–Frat1 (which colocalized with Myc–Dvl1) consistent with a previous report[14]. Both Myc–Dvl1 and GFP–Frat1 localization in the cytosol became diffuse when FLAG–NRX was coexpressed, but this effect was blocked by treatment with H_2O_2; Myc–Dvl1 and GFP–Frat1 colocalize in a punctate pattern again (see Supplementary Information, Fig. S2d). These results suggest that NRX inhibits Wnt–β-catenin signalling by masking the Dvl basic–PDZ domain.

NRX levels were then ablated by RNAi. RNAi of NIH3T3 cells, which contain large amount of NRX compared to other cells, clearly reduced the amount of NRX (Fig. 3a). *NRX* RNAi cells showed elevated TCF activity compared to control RNAi cells, even though the expression level of Dvl was decreased to 69% (Fig. 3b). The upregulation of TCF activity in *NRX* RNAi cells was blocked by expressing a dominant-negative form of TCF (dnTCF) or an NRX construct with two base pairs mutated that prevent interference by the *NRX* RNAi (NRX-esc; see Supplementary Information, Fig. S3a, b). The activities of other transcription factors, serum response factor (SRF) and nuclear factor (NF)-κB, did not change significantly on treatment with *NRX* RNAi (see Supplementary Information, Fig. S3c). Transcription of endogenous c-Myc and Cyclin D1, well-characterized targets of Wnt–β-catenin signalling[15,16], were upregulated in *NRX* RNAi treated cells (Fig. 3c). Taken together, these results indicate that endogenous NRX acts as a suppressor of Wnt–β-catenin signalling.

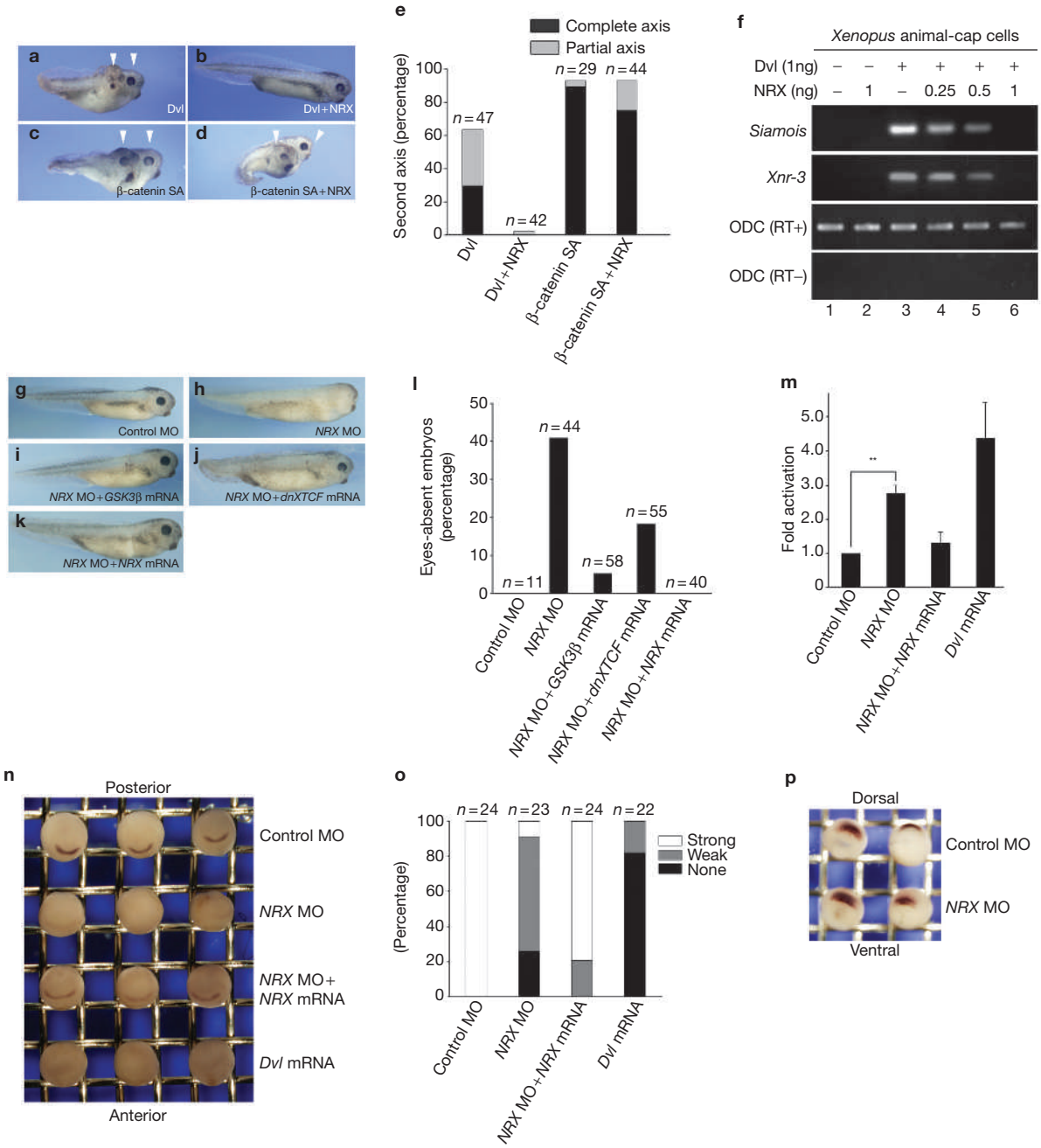

Figure 4 NRX inhibits Wnt–β-catenin signalling in *Xenopus*. (**a**–**d**) Secondary axis formation. The indicated mRNAs were injected into the ventral marginal zone (VMZ) and incubated for 3 days (stage 40). Arrowheads indicate duplicated heads. (**e**) The ratio of secondary axis formation. Complete axis indicates secondary axis formation with head structure. Partial axis indicates ectopic trunk formation with no head. (**f**) Animal-cap cells were excised from embryos injected with *Dvl* and *NRX* mRNA and RT–PCR analyses of the indicated genes was performed. Ornithine decarboxylase (ODC) was used as an internal control. (**g**–**k**) Embryos injected at the animal pole (AP) with the indicated morpholino oligonuleotides and mRNAs. The NRX MO injected embryos have no eyes. This phenotype was rescued by *GSKβ* (**i**), *dnXTCF* (**j**) or *NRX* mRNA (**k**) coinjection. (**l**) The ratio of eyes-absent embryos. (**m**) TCF reporter activities of AP injected embryos. The activities were normalized against that of control MO-injected embryos and results are shown as the mean ± s.e.m. ($n = 4$). Asterisks indicate $P=0.0026$. (**n**) Whole mount *in situ* hybridization of AP injected embryos (stage 15) with probes for *Bf-1*. (**o**) *Bf-1* signal strength was classified and the ratio is indicated. (**p**) Whole mount *in situ* hybridization of AP injected embryos (stage 10.5) with probes for *Chordin*. There was no obvious difference between control and *NRX* MO injected embryos.

BrdU incorporation assays revealed that *NRX* RNAi cells had a higher proliferation rate than control cells (Fig. 3d). Treatment with Wnt3a conditioned media eliminated the difference in proliferation rate, suggesting that the accelerated proliferation of *NRX* RNAi cells was due to activation of Wnt–β-catenin signalling. It is believed that Wnt–β-catenin signalling is involved in tumorigenesis, and that activation of Wnt–β-catenin signalling promotes focus formation by cooperation with activated MEK[17]. Therefore, *NRX* RNAi cells were transfected with HA–MEK–LA–SDSE or FLAG–Ras^{G12V}, constitutively active forms of MEK and Ras, respectively. *NRX* RNAi treated cells formed more foci than control cells (Fig. 3e, f). These results are consistent with an inhibitory function of NRX on Wnt–β-catenin

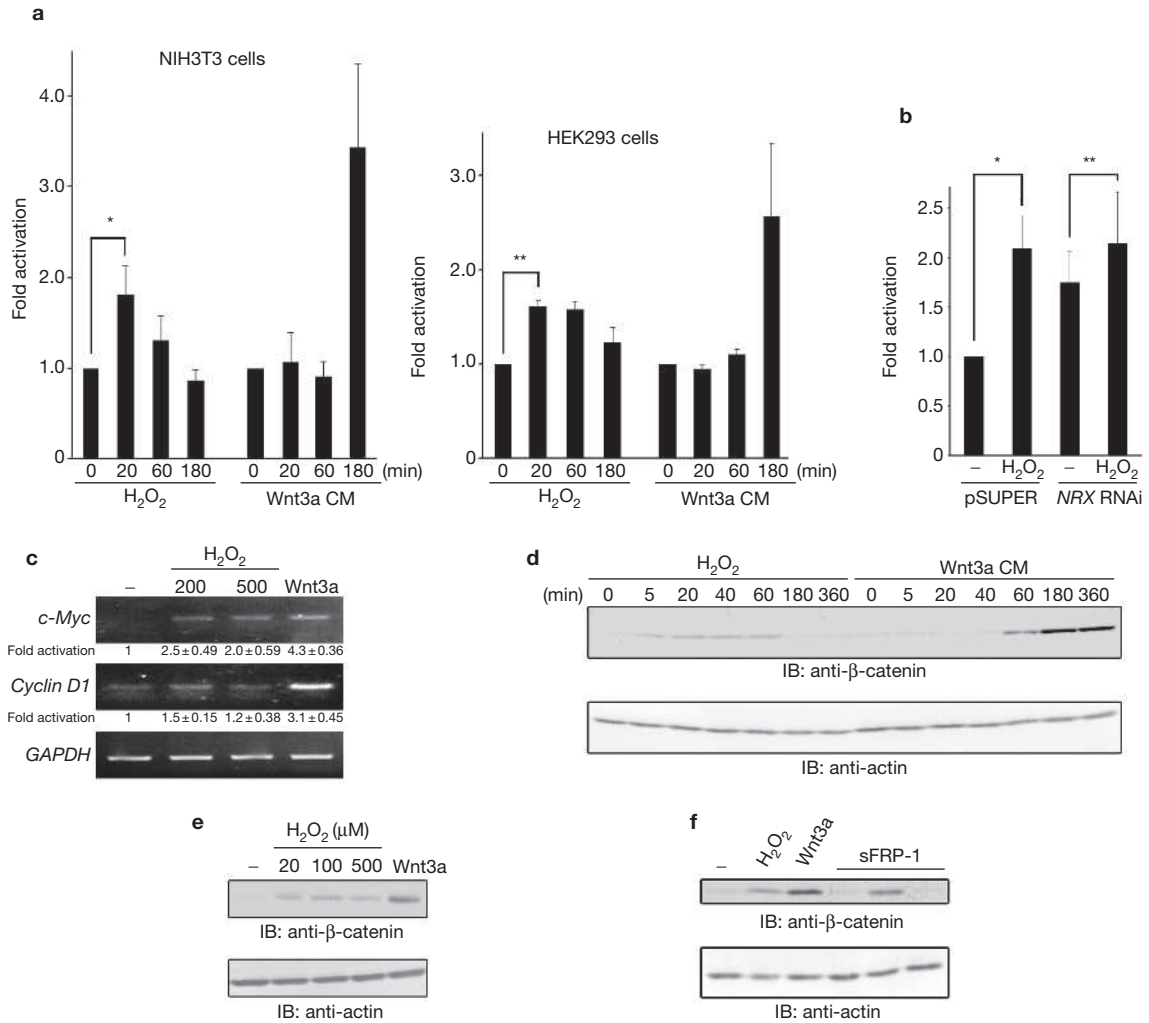

Figure 5 Activation of the Wnt–β-catenin pathway by H_2O_2. (**a**, **b**) TCF reporter activities of H_2O_2-treated (300μM) or Wnt3a CM-treated cells (**a**), or *NRX* RNAi cells treated with H_2O_2 (300μM, 20min; **b**). Results were normalized against the reporter activites of non-treated cells and are shown as the mean ± s.e.m. (**a**, $n = 5$; **b**, $n = 4$). Single and double asterisks indicate $P = 0.024$ and 0.039, respectively in **a**, and indicate $P = 0.030$ and 0.43, respectively in **b**. (**c**) RT–PCR analysis for the indicated genes of NIH3T3 cells treated with H_2O_2 (30min) or Wnt3a CM (3h). The mean ± s.e.m. ($n = 5$) of relative amount of product are also indicated. (**d**–**f**) Immunoblot of lysates from L cells treated with H_2O_2 (200μM) or Wnt3a CM in **d**, H_2O_2 (20min) or Wnt3a CM (3h) in **e**, or 10μg ml^{-1} sFRP-1 followed by H_2O_2 (200μM, 20min) or Wnt3a CM (3h) in **f**. Actin was used as a loading control.

signalling and also suggest that NRX is involved in Wnt-dependent cell proliferation and tumorigenesis.

The function of NRX was confirmed by experiments in *Xenopus laevis* embryos. Injection of a Wnt signalling activator (such as Dvl) to the ventral marginal zone (VMZ) induces ectopic body axis formation[18]. Coinjection of *NRX* mRNA inhibited the secondary axis formation caused by *Dvl* mRNA but not by *β-catenin SA* mRNA (Fig. 4a–e). *Dvl* mRNA injection induced expression of *siamois* and *Xnr-3*, target genes of Wnt–β-catenin signalling in *Xenopus* animal-cap cells, which was blocked by coinjection of *NRX* mRNA (Fig. 4f).

The *in vivo* role of NRX was also examined by injecting antisense morpholino oligonucleotides(MO) of the *Xenopus* NRX homologue, MGC84045 (the protein shows 77% identity with mouse NRX). Injection of *NRX* MO to the animal-pole region caused significant defects in head formation. The eye structures clearly disappeared in *NRX* MO-injected embryos, whereas control MO injected embryos had no obvious defects (Fig. 4g, h, l). Such defective eye phenotypes have been reported when Wnt–β-catenin signalling is abnormally activated in the animal pole region[19–21]. The defect caused by *NRX* MO injection was suppressed by coinjection of *GSK3β*, *dn Xenopus TCF (XTCF)* or *NRX* mRNAs (Fig. 4i–l). The activation of TCF in embryos injected with *NRX* MO was confirmed by reporter assays, and was blocked by coinjection of *NRX* mRNA (Fig. 4m). In addition, the expression of an anterior marker (Bf-1) was clearly suppressed in *NRX* MO injected embryos, but there was no obvious difference in expression of a dorsal marker (Chordin; Fig. 4n–p and see Supplementary Information, Table S1). We concluded that endogenous NRX also functions as a negative regulator of Wnt–β-catenin signalling in *Xenopus*.

NRX negatively regulates Wnt–β-catenin signalling (Figs 2–4) and binds to Dvl in a redox-dependent manner (Fig. 1), suggesting that Wnt–β-catenin signalling is regulated by oxidative stress. NIH3T3 or HEK293 cells treated with H_2O_2 showed modest but significant activation of TCF (Fig. 5a). This H_2O_2-dependent activation of TCF was significantly impaired in *NRX* RNAi cells, indicating the participation of NRX in this

activation (Fig. 5b). Activation of TCF by H_2O_2 was blocked by dnTCF expression (see Supplementary Information, Fig. S3d). RT–PCR analyses showed upregulation of endogenous c-Myc and Cyclin D1 in cells treated with H_2O_2 and in cells treated with Wnt3a conditioned media (Fig. 5c). The accumulation of β-catenin was also observed in L cells, in which β-catenin accumulation was quantitatively examined by immunoblotting (Fig. 5d). β-catenin accumulation occured at 20–500 μM H_2O_2 and persisted for 5–60 min after stimulation (Fig. 5e). In contrast, Wnt3a conditioned media-dependent activation occured 3 h after treatment. Pretreatment of cells with sFRP-1, a secreted Wnt antagonist[22,23], completely inhibited β-catenin accumulation induced by Wnt3a conditioned media, but not by H_2O_2 (Fig. 5f). These results suggest that oxidative stress augments Wnt–β-catenin signalling by directly affecting the intracellular signalling machinery and that the redox-dependent interaction between Dvl and NRX is important for the activation of Wnt–β-catenin signalling by H_2O_2.

Intense oxidative stress induces cell-cycle arrest or apoptosis. At a moderate level, however, oxidative stress accelerates proliferation[24] and growth factors can stimulate the generation of ROS[25], which are essential for proliferative responses through various signalling intermediates[26,27]. Furthermore, there are many reports showing high levels of ROS in various tumour cells. It is likely that redox-dependent regulation of Wnt–β-catenin signalling through NRX contributes to cell proliferation induced by oxidative stress. □

METHODS

Constructs. Amino-acid positions of the deletion constructs for human Dvl1 and mouse NRX are as follows: Dvl1–DIX (DIX, Dishevelled–Axin; 1–160), basic–PDZ (140–379), PDZ (234–379), basic (140–256), DEP–CT (302–670), PDZ–DEP (67–499), ΔCT (1–517), NRX–C1 (162–435), Redox (193–297), C2 (302–435). NRX^{C205S} and NRX^{C208S} mutants, and NRX-esc (T1068C, C1071A, no change in amino acids) were generated with a QuickChange site-directed mutagenesis kit (Stratagene, La Jolla, CA). MEK–LA–SDSE, Ras^{G12V}, β-catenin SA, GSK3β, ΔN90-β-catenin, dnXTCF, wtTCF, and dnTCF were generated as described previously[9,14,21,28–30].

Cells. L-Wnt3a cells were purchased from American Type Cell Collection (Manassas, VA). COS7, HEK293, L, N1E-115 and BOSC23 cells were maintained routinely in DMEM with 10% fetal bovine serum and antibiotics. NIH3T3 cells were cultured in DMEM plus 10% calf serum and antibiotics.

Proteins. Recombinant sFRP-1 protein was obtained from R&D Systems (Minneapolis, MN). GST–Dvl1–PDZ–DEP–His and GST–NRX were expressed in Sf9 insect cells and purified with glutathione–Sepharose 4B beads (Amersham, Piscataway, NJ). His–Frat1 and His–NRX were expressed in Sf9 cells and *Escherichia coli*, respectively, and purified with Ni–NTA beads (Qiagen, Hilden, Germany).

Antibodies. Mouse anti-Lamin B, mouse anti-tubulin and anti-Myc (mouse monoclonal and rabbit polyclonal) antibodies were obtained from Santa Cruz Biotechnology (Santa Cruz, CA). Commercially available antibodies were also used for β-catenin (mouse monoclonal from BD Biosciences, San Jose, CA), actin (mouse monoclonal from Invitrogen, Carlsbad, CA), and FLAG (mouse monoclonal and rabbit polyclonal from Sigma-Aldrich, St Louis, MO). Anti-Dvl, anti-NRX and anti-NRX(N) rabbit polyclonal antibodies were all generated using recombinant proteins (amino acids 1–222 for the anti-Dvl antibody and amino acids 1–121 for the anti-NRX(N) antibody) and were affinity purified. Full-length NRX was used to raise anti-NRX antibodies, which were purified with C-terminal region of NRX (amino acids 162–435). Anti-Frat antisera was generated in rabbits immunized with recombinant Frat1 proteins (amino acids 132–279).

Identification of proteins. Proteins bound to the anti-FLAG M2 agarose beads (Sigma) were separated by SDS–PAGE and visualized by CBB staining. Bands of interest were excised from the gels and the proteins in each gel slice were digested with trypsin. The trypsinized peptides were then extracted from the gels with acetonitrile containing 5% formic acid and 0.1% trifluoroacetic acid. The peptides were subjected to liquid chromatography for purification, and were analysed by matrix-assisted laser desorption-ionization/time of flight–mass-spectrometry/mass-spectrometry (MALDI/TOF–MS/MS; 4700 Proteomics Analyzer; Applied Biosystems, Foster City, CA). Detected masses and the sequences of the peptides were subjected to database searches with the Mascot search engine (Matrix Science, London, UK).

Reporter assays. The reporter plasmids TOPFLASH, FOPFLASH (Upstate, Chicago, IL), pSRF–Luc and pNF-κB–Luc (Stratagene) were used in this study. pTK–RL (Promega, Madison, WI) was used as an internal control. Cultured cells were transfected with FuGENE6 (Roche, Indianapolis, IN) and harvested 48 h after transfection. Reporter activities were measured with a plate reader (LD400; Beckman Coulter, Fullerton, CA) using a dual luciferase reporter assay system (Promega). TCF/LEF activity was defined as the ratio of TOPFLASH:FOPFLASH reporter activities. Each assay was performed in duplicate and all results are shown as the mean ± s.e.m. of at least three independent assays.

***Xenopus* experiments.** mRNA synthesis, microinjection, RT–PCR analyses and whole mount *in situ* hybridization experiments were performed as previously described[21]. Briefly, mRNA was generated by mMessage mMachine kit (Ambion, Austin, TX). Fertilized eggs were injected at the four-cell stage (ventral marginal zone) or eight-cell stage (animal pole). The embryos were then cultured in 10% Steinberg's solution for 3 days before examination. For RNA extraction, animal-cap cells were dissected at stage 8.5, cultured for 1 h and then harvested. RNA isolation was performed with ISOGEN (Nippon Gene, Tokyo, Japan). The sequence and conditions for each primer set used for RT–PCR are as follows: *XODC* (5′-GTCAATGATGGAGTGTATGGATC-3′ and 5′-TCCATTCCGCTCTCCTGAGCAC-3′; annealing temperature = 58 °C, 28 cycles), *Siamois* (5′-AAGATAACTGGCATTCCTGAG C-3′ and 5′-GGTAGGGCTGTGTATTTGAAGG-3′, annealing temperature = 56 °C, 30 cycles) and *Xnr3* (5′-CTTCTGCACTAGATTCTG-3′ and 5′-CAGCTTCTGGCCAAGACT-3′, annealing temperature = 58 °C, 28 cycles). Morpholino antisense-oligonucleotides were from Gene Tools (Philomath, OR). The sequence of the morpholino oligonucleotides were as follows: *NRX* MO (GCCTGGCCCCACCTCTCTTCTGTGT); control MO (CCTCTT ACCTCAGTTACAATTTATA). *NRX* MO (7.5 ng), control MO (20 ng) and 1 ng of each mRNA was injected per embryo unless otherwise indicated. For luciferase assays, eggs were injected at the animal pole region with TOPFLASH or FOPFLASH (Upstate) plus pTK–RL (Promega). The embryos were harvested at stage 13 and the reporter activities were measured by 20/20^n luminometry system (Promega). TCF/LEF activity was defined as the ratio of TOPFLASH:FOPFLASH reporter activities. Each assay was performed in duplicate and all results are shown as the mean ± s.e.m. of four independent assays.

RNA interference assays. The following sequence, derived from mouse *NRX* cDNA was used for RNAi assays: (AA)GATCATTGCCAAGTACAAA (1060–1080). For control RNAi, the following sequence was used: (AA)GATCATTGCACAGTACAAA (the two underlined nucleotides are inverted relative to the *NRX* RNAi sequence). pCL–Ampho (Imgenex, San Diego, CA) and oligonucleotide-inserted pSUPER–RETRO vectors (OligoEngine, Seattle, WA) were cotransfected into BOSC23 cells using FuGENE6 to generate retrovirus. Culture supernatants containing recombinant retrovirus were used to infect NIH3T3 cells. Retrovirus-infected cells were selected with puromycin. Positive NRX signals could not be detect ed in lysates from *NRX* RNAi cells up to 40 days after puromycin selection.

RT–PCR analysis. RNA from cultured cells was prepared with ISOGEN (Nippon Gene) and cDNA was synthesized from 2 μg RNA with Revertra ace (Toyobo, Osaka, Japan). The primers used were as follows; *GAPDH* (5′-CTCTTCCACCTTCGATGCC-3′ and 5′-GGGGAGATGCTAGTGCTCTTG-3′), and *Cyclin D1* (5′-CATCAAGTGTGACCCGGACTG-3′ and 5′-CCTCCTCCTCAGTGGCCTTG-3′). The conditions (annealing temperature = 60 °C, 23 cycles for *GAPDH* and *c-Myc*, and annealing temperature = 64 °C, 25 cycles for *Cyclin D1*) were chosen so that none of the amplified DNAs reached a plateau. The amount of amplified cDNAs was

densitometically quantified and normalized against GAPDH. The mean ± s.e.m. of five independent assays are shown.

Statistics All statistical analyses are shown as mean ± s.e.m. of independent multiple assays. Significance was determined by two-tailed Student's *t* test or ANOVA (Fig. 5a).

Note: Supplementary Information is available on the Nature Cell Biology website.

ACKNOWLEDGEMENTS

We thank S. Ohmi and H. Fukuda for mass spectrometry analysis. We are grateful to R. J. Davis for JNK1, S. Yokoyama for Ras^{G12V}, E. Nishida for HA–MEK LA SDSE, Y. Furukawa and Y. Nakamura for wild-type TCF-4 and dominant negative TCF-4, and Y. Gotoh for β-catenin and c-Jun. We also appreciate helpful advice and support from T. Takenawa, K. Takenaka, H. Yamaguchi, T. Terabayashi, A. Yukita, K. Haraguchi, S. Aizawa and T. Chano. This study was supported in part by a Grant-in-Aid for Cancer Research from the Ministry of Education, Science, and Culture of Japan.

COMPETING FINANCIAL INTERESTS

The authors declare that they have no competing financial interests.

Published online at http://www.nature.com/naturecellbiology/
Reprints and permissions information is available online at http://npg.nature.com/reprintsandpermissions/

1. Nelson, W.J. & Nusse, R. Convergence of Wnt, β-catenin, and cadherin pathways. *Science* **303,** 1483–1487 (2004).
2. Reya, T. & Clevers, H. Wnt signalling in stem cells and cancer. *Nature* **434,** 843–850 (2005).
3. Moon, R.T., Kohn, A.D., De Ferrari, G.V. & Kaykas, A. WNT and β-catenin signalling: diseases and therapies. *Nature Rev. Genet.* **5,** 691–701 (2004).
4. Kurooka, H. *et al.* Cloning and characterization of the nucleoredoxin gene that encodes a novel nuclear protein related to thioredoxin. *Genomics* **39,** 331–339 (1997).
5. Laurent, T.C., Moore, E.C. & Reichard, P. Enzymatic synthesis of deoxyribonucleotides. IV. Isolation and characterization of thioredoxin, the hydrogen donor from *Escherichia coli* B. *J. Biol. Chem.* **239,** 3436–3444 (1964).
6. Chae, H.Z. *et al.* Cloning and sequencing of thiol-specific antioxidant from mammalian brain: alkyl hydroperoxide reductase and thiol-specific antioxidant define a large family of antioxidant enzymes. *Proc. Nat. Acad. Sci. USA* **91,** 7017–7021 (1994).
7. Saitoh, M. *et al.* Mammalian thioredoxin is a direct inhibitor of apoptosis signal-regulating kinase (ASK) 1. *EMBO J.* **17,** 2596–2606 (1998).
8. Yanagawa, S., van Leeuwen, F., Wodarz, A., Klingensmith, J. & Nusse, R. The dishevelled protein is modified by wingless signaling in *Drosophila*. *Genes Dev.* **9,** 1087–1097 (1995).
9. Barth, A.I., Pollack, A.L., Altschuler, Y., Mostov, K.E. & Nelson, W.J. NH2-terminal deletion of β-catenin results in stable colocalization of mutant β-catenin with adenomatous polyposis coli protein and altered MDCK cell adhesion. *J. Cell Biol.* **136,** 693–706 (1997).
10. Li, L. *et al.* Dishevelled proteins lead to two signaling pathways. Regulation of LEF-1 and c-Jun N-terminal kinase in mammalian cells. *J. Biol. Chem.* **274,** 129–134 (1999).
11. Moriguchi, T. *et al.* Distinct domains of mouse dishevelled are responsible for the c-Jun N-terminal kinase–stress-activated protein kinase activation and the axis formation in vertebrates. *J. Biol. Chem.* **274,** 30957–30962 (1999).
12. Yost, C. *et al.* GBP, an inhibitor of GSK-3, is implicated in *Xenopus* development and oncogenesis. *Cell* **93,** 1031–1041 (1998).
13. Li, L. *et al.* Axin and Frat1 interact with dvl and GSK, bridging Dvl to GSK in Wnt-mediated regulation of LEF-1. *EMBO J.* **18,** 4233–4240 (1999).
14. Hino, S., Michiue, T., Asashima, M. & Kikuchi, A. Casein kinase Iε enhances the binding of Dvl-1 to Frat-1 and is essential for Wnt-3a-induced accumulation of β-catenin. *J. Biol. Chem.* **278,** 14066–14073 (2003).
15. He, T.C. *et al.* Identification of c-MYC as a target of the APC pathway. *Science* **281,** 1509–1512 (1998).
16. Tetsu, O. & McCormick, F. β-catenin regulates expression of cyclin D1 in colon carcinoma cells. *Nature* **398,** 422–426 (1999).
17. Rimerman, R.A., Gellert-Randleman, A. & Diehl, J.A. Wnt1 and MEK1 cooperate to promote cyclin D1 accumulation and cellular transformation. *J. Biol. Chem.* **275,** 14736–14742 (2000).
18. Sokol, S.Y., Klingensmith, J., Perrimon, N. & Itoh, K. Dorsalizing and neuralizing properties of Xdsh, a maternally expressed *Xenopus* homolog of dishevelled. *Development* **121,** 1637–1647 (1995).
19. Kim, C.H. *et al.* Repressor activity of Headless–Tcf3 is essential for vertebrate head formation. *Nature* **407,** 913–916 (2000).
20. Kiecker, C. & Niehrs, C. A morphogen gradient of Wnt–β-catenin signalling regulates anteroposterior neural patterning in *Xenopus*. *Development* **128,** 4189–4201 (2001).
21. Michiue, T. *et al.* XIdax, an inhibitor of the canonical Wnt pathway, is required for anterior neural structure formation in *Xenopus*. *Dev. Dyn.* **230,** 79–90 (2004).
22. Leyns, L., Bouwmeester, T., Kim, S.H., Piccolo, S. & De Robertis, E.M. Frzb-1 is a secreted antagonist of Wnt signaling expressed in the Spemann organizer. *Cell* **88,** 747–756 (1997).
23. Wang, S., Krinks, M., Lin, K., Luyten, F.P. & Moos, M., Jr. Frzb, a secreted protein expressed in the Spemann organizer, binds and inhibits Wnt-8. *Cell* **88,** 757–766 (1997).
24. Burdon, R.H. & Rice-Evans, C. Free radicals and the regulation of mammalian cell proliferation. *Free Radic. Res. Commun.* **6,** 345–358 (1989).
25. Sundaresan, M., Yu, Z.X., Ferrans, V.J., Irani, K. & Finkel, T. Requirement for generation of H_2O_2 for platelet-derived growth factor signal transduction. *Science* **270,** 296–299 (1995).
26. Finkel, T. Oxidant signals and oxidative stress. *Curr. Opin. Cell Biol.* **15,** 247–254 (2003).
27. Rhee, S.G. *et al.* Intracellular messenger function of hydrogen peroxide and its regulation by peroxiredoxins. *Curr. Opin. Cell Biol.* **17,** 183–189 (2005).
28. Miki, H., Fukuda, M., Nishida, E. & Takenawa, T. Phosphorylation of WAVE downstream of mitogen-activated protein kinase signaling. *J. Biol. Chem.* **274,** 27605–27609 (1999).
29. Molenaar, M., *et al.* XTcf-3 transcription factor mediates β-catenin-induced axis formation in *Xenopus* embryos. *Cell* **86,** 391–399 (1996).
30. Fujita, M. *et al.* Up-regulation of the ectodermal-neural cortex 1 (*ENC1*) gene, a downstream target of the β-catenin–T-cell factor complex, in colorectal carcinomas. *Cancer Res.* **61,** 7722–7726 (2001).

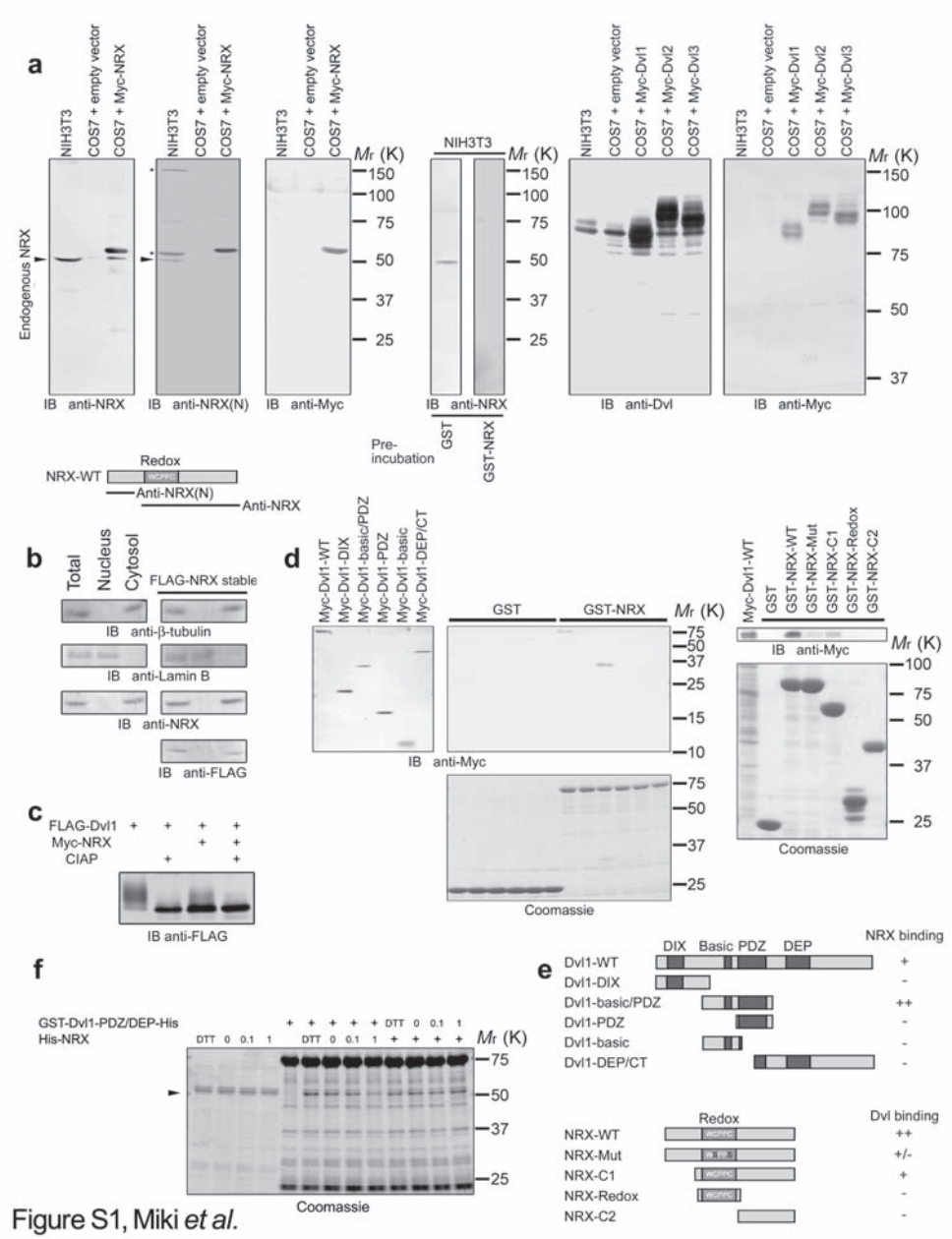

Figure S1, Miki *et al.*

Figure S1 Characterization of Dvl/NRX complex. (a) Left: Expressed or endogenous NRX detected by immunoblotting with two anti-NRX antibodies from distinct epitope regions (anti-NRX and anti-NRX(N)). *Arrowheads*: endogeneous NRX, *asterisks*: non-specific bands. Middle: Immunoblotting by anti-NRX antibodies preincubated with 10-fold moler excess GST/GST-NRX (immobilized). Right: Overexpressed FLAG-Dvl1-3 and endogenous Dvl detected by immunoblotting with anti-Dvl antibody. (b) Lysates from NIH3T3 cells and NIH3T3 cells stably expressing FLAG-NRX were separated into nuclear and cytosolic fractions. (c) Anti-FLAG immunoprecipitates of expressed COS7 cell lysates were treated with calf intestine-derived alkaline phosphatase (CIAP). (d) Left: Transfected COS7 cell lysates were subjected to pull-down assays by GST/GST-NRX. Right: Myc-Dvl1 expressing COS7 cell lysates were used for pull-down assays with GST/GST-tagged NRX (-WT, -Mut, -C1, -redox, or -C2). (e) Wild-type and mutants of Dvl and NRX. Binding to NRX or Dvl1 is indicated as + (positive) and - (negative). (f) GST-Dvl1-PDZ/DEP-His and His-NRX were selectively treated with DTT (1 mM) or H_2O_2 (0.1 or 1 mM), and subjected to pull-down assays. Bound His-NRX was detected by CBB staining. *Arrowhead*: His-NRX.

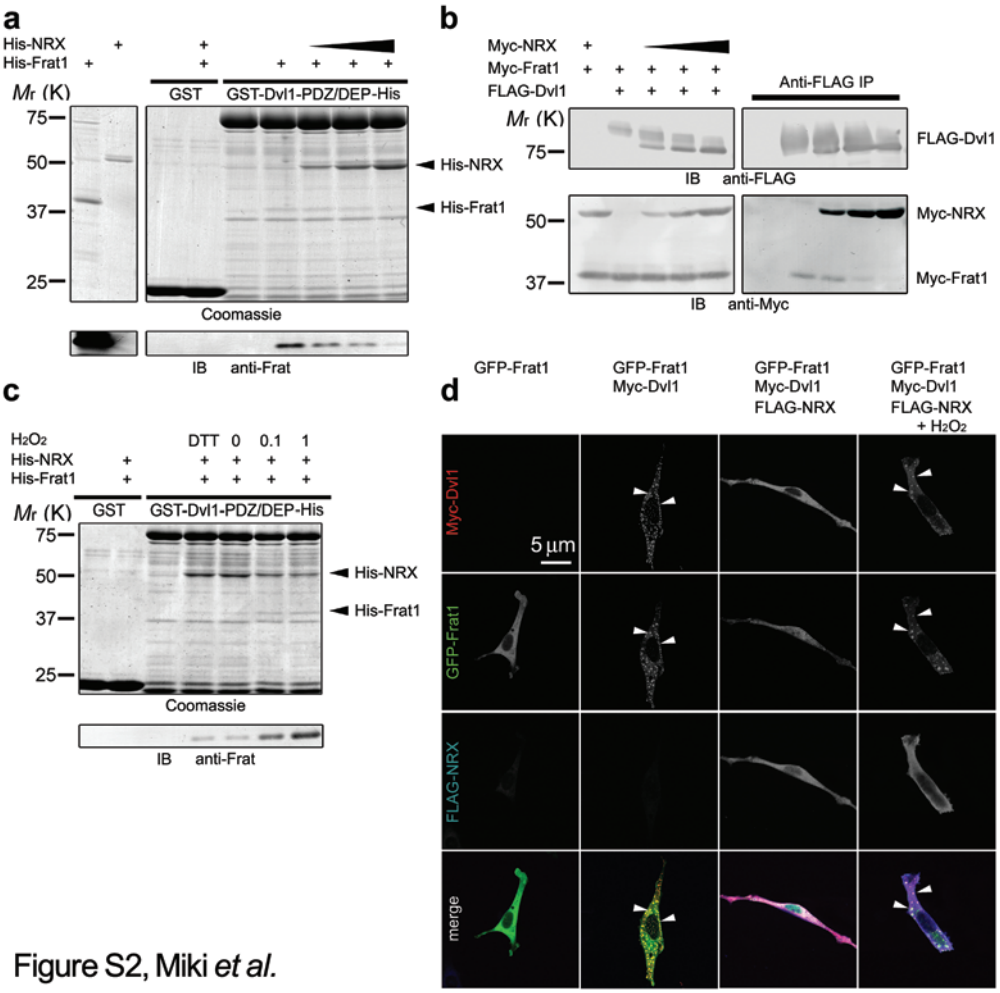

Figure S2, Miki *et al.*

Figure S2 Competition between NRX and Frat for Dvl. (a) His-Frat1 (1 μM) and His-NRX (0.3, 1.0, or 3.0 μM) were mixed with immobilized GST-Dvl1-PDZ/DEP-His. (b) Transfected COS7 cell lysates were subjected to anti-FLAG IP. (c) His-Frat1 (1 μM) and His-NRX (1 μM) were incubated with immobilized GST-Dvl1-PDZ/DEP-His under reduced (1 mM DTT) or oxidized (H_2O_2) conditions. (d) Transfected NIH3T3 cells were treated with H_2O_2 (1 mM, 1 h). Red: anti-Myc (Dvl1), Green: GFP (Frat), Blue: anti-FLAG (NRX). *Arrowheads*: Myc-Dvl1 or GFP-Frat1 showing vesicular localization.

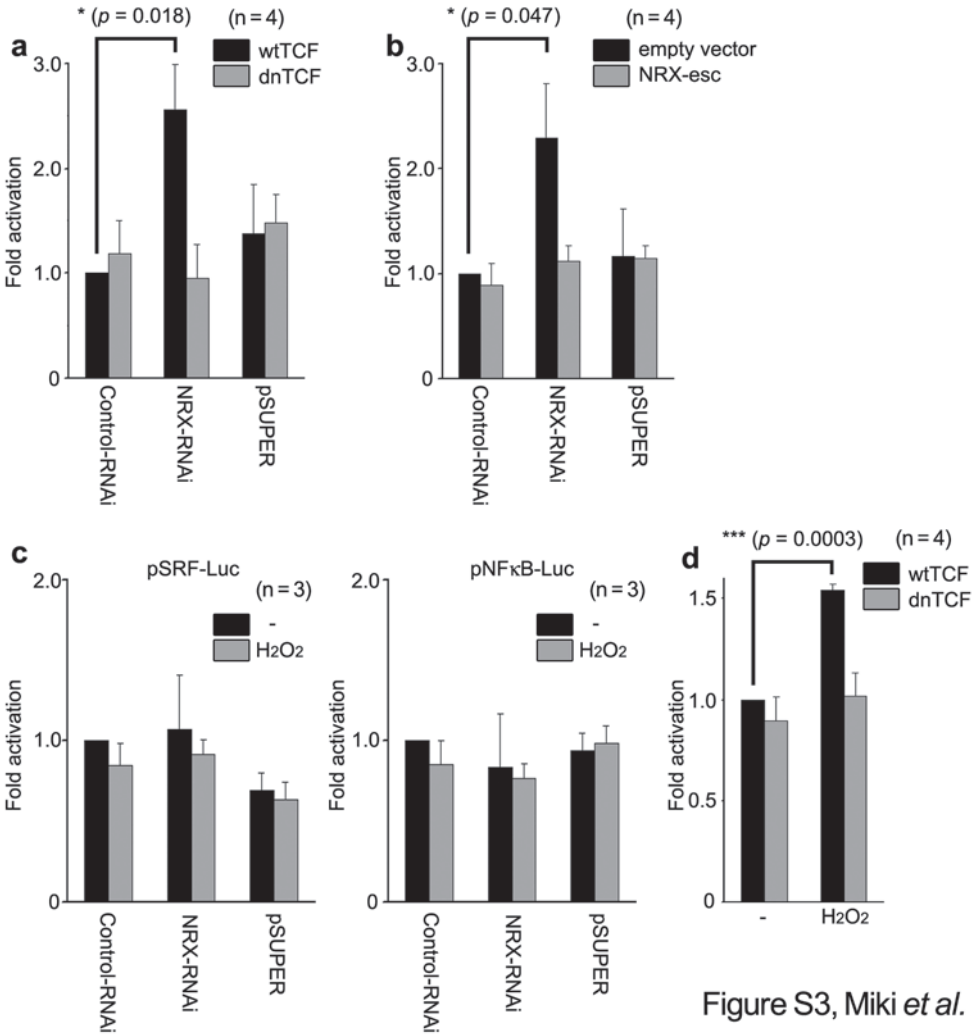

Figure S3 Control experiments for luciferase assays. NRX-RNAi cells and control cells were transfected with (a), wtTCF/dnTCF or (b), NRX-esc, and TCF/LEF activities were determined. (c), NRX-RNAi cells and control cells were treated with H_2O_2 (300 μM, 20 min) and the activities of SRF and NFκB were determined. (d), NIH3T3 cells transfected with wtTCF or dnTCF were treated with H_2O_2 (300 μM, 20 min), and TCF/LEF activities were determined.

Table S1 Quantified results of whole mount *in situ* hybridization experiments.

Bf-1	Strong	Weak	None	Total
Control MO	24	0	0	24
NRX-MO	2	15	6	23
NRX-MO + NRX mRNA	19	5	0	24
Dvl mRNA	0	4	18	22

Chordin	Strong	Weak	None	Total
Control MO	14	0	0	14
NRX-MO	10	0	0	10

Strong: Positive signal can be clearly observed.
Weak: Severely suppressed compared to the “Strong” group, but positive signal can still be observed. None: No positive signal can be observed.